Theoretical Studies of the Hydrolysis of the Methyl Phosphate Anion

Ching-Han Hu[†] and Tore Brinck*[,‡]

Physical Chemistry, Royal Institute of Technology, SE-10044 Stockholm, Sweden

Received: August 25, 1998; In Final Form: December 28, 1998

The mechanism for the hydrolysis of the methyl phosphate anion was studied using high-level ab initio and density functional theory methods. Starting from the molecular species $CH_3OPO_3H^-$, $CH_3OPO_3H^-\cdot(H_2O)$, and $CH_3OPO_3H^-\cdot(H_2O)_2$, gas phase reaction coordinates of the proposed mechanisms were followed. Solvation free energies were evaluated using the polarizable continuum model (PCM) at the stationary point geometries. The dissociative mechanism, which involves the formation of a metaphosphate ion (PO_3^-), is found to be more favorable than the associative mechanism, which involves a pentacoordinated intermediate, both in the gas phase and in aqueous solution. In the dissociative mechanism, the first step is rate determining. The computed free energy of activation in solution is within 1.7 kcal/mol of the experimentally determined activation free energy for hydrolysis. The first step and the second step in the dissociative mechanism are each shown to proceed via a six-centered water-assisted transition state.

Introduction

The hydrolysis of phosphate esters is one of the most important biochemical processes in living systems.[1] The biological energy reservoir adenosine triphosphate (ATP) transfers its terminal phosphoryl group to various substrates. The genetic materials DNA and RNA are phosphodiesters, and their stabilities are dependent upon the activation energies for the hydrolysis of phosphate esters. Despite the great importance of phosphate ester reactions, the mechanism for the hydrolysis of methyl phosphate, the simplest phosphate ester, is still not well understood. In this work, we focus on the hydrolysis of the methyl phosphate anion, which is the major species in aqueous solutions of methyl phosphate in the pH range 2−7.

The maximum rate for the hydrolysis of methyl phosphate is 8×10^{-6} s^{-1} at 373 K and pH = 4.2.[2] It was proposed in 1955 that the mechanism is dissociative and involves the formation of an intermediate monomeric "metaphosphate" ion (PO_3^-) in the first step.[3,4] The intermediate then reacts with a solvent water molecule which act as a nucleophile to yield the orthophosphoric acid monoanion ($H_2PO_4^-$).

$$CH_3OPO_3H^- \rightarrow [PO_3^-] + CH_3OH \qquad (1a)$$

$$[PO_3^-] + H_2O \rightarrow H_2PO_4^- \qquad (1b)$$

It has been debated whether PO_3^- exists as a free diffusable species in water.[5] Kinetic and stereochemical studies have indicated that free PO_3^- intermediates cannot be generated in protic solvent.[6−9] Lightcap and Frey concluded that PO_3^- is too reactive and cannot escape its aqueous solvation sphere.[10] Keesee and Castleman found $PO_3^-\cdot(H_2O)_n$ clusters with up to two water molecules to be stable in the gas phase.[11] However, addition of a third water molecule leads to isomerization of the cluster into the dihydrate of $H_2PO_4^-$ [$H_2PO_4^-$ $(H_2O)_2$]. The stability of $PO_3^-\cdot(H_2O)_n$ clusters and their isomerization to $H_2PO_4^-\cdot(H_2O)_{n-1}$ have also been investigated in two independent quantum chemical studies.[12,13] In both studies it was found that the activation barrier for isomerization decreases with the number of water molecules. In particular, there is a significant decrease in the barrier when going from a cluster with one to two water molecules. The isomerization of $PO_3^-\cdot(H_2O)_2$ proceeds via a six-centered water-assisted transition state which is considerably lower in energy than the four-centered transition state that is formed during the isomerization of $PO_3^-\cdot(H_2O)$.[12,13] In conclusion, both the available experimental and theoretical data suggest that the barrier for reaction 1b should be rather low in aqueous solution. However, it cannot be excluded that reaction 1b is rate determining, since this depends not only of the activation free energy of this reaction but also on the relative free energy of the hydrated PO_3^-.

An alternative mechanism for the hydrolysis of methyl phosphate involves the formation of a pentacoordinated trigonal-bipyramidal (TBP) intermediate:[14,15]

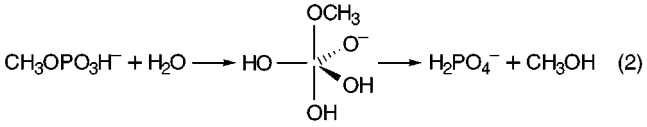

(2)

This associative mechanism is similar to the mechanism for hydrolysis of esters of carboxylic acids, in which tetrahedral intermediates are formed during the reaction. It has been pointed out by Westheimer that ligands may only enter or leave the TBP intermediate apically.[14] The noninline TBP intermediate that has an equatorial leaving group will have to undergo at least one pseudorotation before completing the reaction.

In a recent theoretical study, Florian and Warshel investigated the energetics of the associative and dissociative mechanisms for phosphate ester hydrolysis.[16] The gas phase reaction coordinates of the two mechanisms were calculated at the ab initio HF/6-31G* level of theory. Electron correlation effects on the potential energy surface were accounted for by single-point calculations at the MP2/6-31+G** level. The solvation effects on the energetics were computed using a Langevin

[†] Present address: Department of Chemistry, National Changhua University, Changhua 50058, Taiwan.

[‡] E-mail: tore@physchem.kth.se.

10.1021/jp9835061 CCC: $18.00
Published on Web 06/15/1999

dipoles model for the solvent. The activation energies reported in this study suggest that the associative and dissociative mechanisms should be of near equal importance in the hydrolysis of the methyl phosphate anion. However, it should be noted that the computed activation energies are more than 7 kcal/mol higher than the experimental estimate of the activation energy. There may be several reasons for this discrepancy between theory and experiment. First of all, it is questionable if the computational level is appropriate for a quantitative analysis of the potential energy surface. Second, and more important, Florian and Warshel have not considered the participation of water molecules from the first solvation shell in the reactions. We have already mentioned that the computed activation energy for reaction 1b is lowered significantly when two water molecules are allowed to play an active role in the reaction. Similar effects may also be important in the other steps of the two mechanisms and lead to significantly lower activation energies.

In a study prior to the one discussed above, Florian and Warshel suggested that the associative reaction may proceed via proton transfer from a water molecule to the phosphate oxygen, followed by nucleophilic attack of OH^- on the phosphorus center to yield the TBP intermediate:[17]

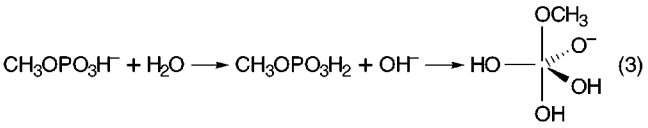

(3)

The dissociation of the TBP intermediate could proceed either via a methoxide ion or according to the regular associative mechanism. As has been emphasized by Florian and Warshel, the transition states for the regular associative mechanism and the "OH^- attack mechanism" are very similar.[16] This makes it hard to distinguish between the two mechanisms using computational methods. Unfortunately, it is also very difficult to set up an experiment that allows the two mechanisms to be distinguished.[16]

In this study we have reinvestigated the energetics of the associative and dissociative mechanisms for hydrolysis of the methyl phosphate anion. In order to determine the importance of first solvation shell effects, the reactions have been studied for the molecular species $CH_3OPO_3H^-$, $CH_3OPO_3H^-\cdot(H_2O)$, and $CH_3OPO_3H^-\cdot(H_2O)_2$. Gas phase energies have been calculated using correlated methods and large basis sets. Nonspecific solvation effects have been included by means of a polarizable continuum model (PCM).

Methods and Procedure

Molecular geometries of stationary points, i.e., minima (initial complexes, intermediates, and products) and transition states involved in the hydrolysis of the methyl phosphate anion were fully optimized at the HF/6-31+G* level of theory. Minima and transition states were further characterized by vibrational frequency analysis. Starting from the HF/6-31+G* structures and analytic Hessians, we have also optimized all stationary points using density functional theory at the B3LYP/6-31+G* level. The combination of Becke's three-parameter mixing of exchange (B3)[18] and the Lee−Yang−Parr correlation (LYP)[19] functional has been shown to provide accurate geometries and reaction energies.[20−22] The B3LYP functional has also been found to perform well for prediction of activation energies.[23−26] However, some studies indicate that B3LYP consistently underestimates the barriers for certain types of reactions, such as open shell and proton transfer reactions.[24,25] For comparison, we have therefore also computed MP2/6-31+G** energies at the B3LYP/6-31+G* optimized geometries. Finally, the activation energies for the rate-limiting steps of the two investigated reaction pathways were computed using a G2 type of scheme:[27]

$$\Delta E = \Delta E[\text{MP2/6-311+G(2df,2p)}] - \Delta E[\text{MP2/6-31+G*}] + \Delta E[\text{CCSD(T)/6-31+G*}] \quad (4)$$

The B3LYP/6-31+G* optimized geometries were used for the MP2 and CCSD(T) calculations. This scheme provides an effective approach for estimating relative CCSD(T)/6-311+G(2df,2p) energies. It should be noted that the empirical correction used in regular G2 theory are not needed here,[27] since we only work with closed-shell species and since the total number of electrons are not changed during the reactions. On the basis of earlier studies using similar schemes, we expect that this procedure can produce activation energies with an accuracy of 2−3 kcal/mol.[27−29]

Harmonic vibrational frequencies obtained at the HF/6-31+G* level were scaled by 0.89 to account for anharmonicity and electron correlation effects. These frequencies were used in the calculations of thermodynamic quantities including zero-point vibrational energies (ZPVE), temperature corrections of molecular vibrations, and vibrational entropies. In order to calculate gas phase free energies, temperature corrections were also made for rotational and translational movements.

Solvation free energies were calculated at the HF/6-31+G* level using a recent version of the polarizable continuum model (PCM/DIR)[30] implemented in the GAMESS program.[31] The new approach developed by Mennuci and Tomasi for renormalization of the apparent charge distribution due to the molecular charge distribution lying outside the solute cavity was used.[32] Following the recommendations of Cossi et al.,[30] we used the Pauling set of atomic radii in the calculations (C = 1.5 Å, N = 1.5 Å, O = 1.4 Å, and H = 1.2 Å). However, for P we used a slightly larger radius than recommended by Pauling, 1.9 Å instead of 1.8 Å, since we found this value to give better agreement with experimental solvation energies for anions containing phosphorus. We did not calculate the cavitation, repulsion, or dispersion contributions to the solvation energies. It has been shown that such contributions are necessary to include in order to reproduce absolute solvation energies.[33] However, the sizes of these contributions correlate strongly with molecular size (surface area or molecular volume).[33] Thus, since the reactions in this study are studied in unimolecular clusters whose sizes remain nearly constant, it can be expected that the contributions from cavitation, repulsion and dispersion on the relative solvation energies are small. The final relative free energies in solution were calculated as the sum of the gas phase free energies and the solvation energies.

The Gaussian 94 suite of programs was used for the gas phase ab initio and DFT computations reported in this study.[34] The GAMESS software (version 6 Jan. 1998) was used for the calculation of PCM solvation energies.[31]

Results

We followed the reaction coordinates of the dissociative mechanism (eq 1) and the associative mechanism (eq 2), and characterized minima and transition states by frequency calculations. The reactions were carried out for the molecular species $CH_3OPO_3H^-$, $CH_3OPO_3H^-\cdot(H_2O)$, and $CH_3OPO_3H^-\cdot(H_2O)_2$. For each species, the second step of the dissociative mechanism involves exchanging the methanol formed in the reaction for

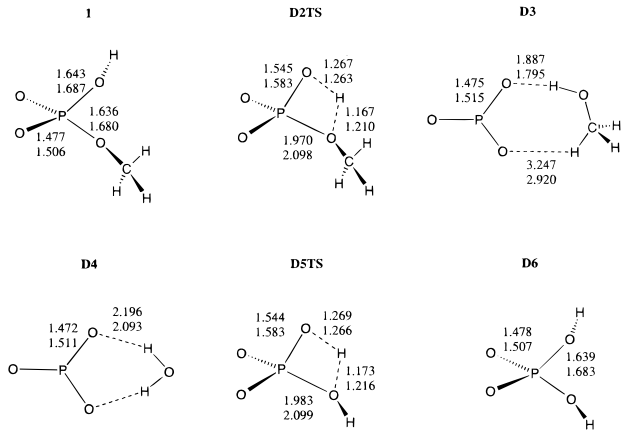

Figure 1. Structures of the stationary points involved in the reaction of $CH_3OPO_3H^-$. The first and second entries of the selected bond lengths (in Å) are computed at the HF/6-31+G* and B3LYP/6-31+G* levels of theory, respectively.

an additional water molecule. The computational results are presented in the order of stoichiometries.

1. Reaction of CH_3OPO_3H in the Dissociative Mechanism. For the $CH_3OPO_3H^-$ species, the only possible reaction is to yield PO_3^- in the dissociative mechanism via a four-centered transition state. The structures of stationary points involved in this mechanism are illustrated in Figure 1 with selected geometrical parameters. The minimum of $CH_3OPO_3H^-$ (**1**) first undergoes proton transfer to the methoxy oxygen via a four-centered transition state (**D2TS**) and forms a molecular complex of PO_3^- and methanol (**D3**). The methanol is then exchanged for a water molecule, which gives a $PO_3^-\cdot H_2O$ complex (**D4**). This complex isomerize to $H_2PO_4^-$ (**D6**) via a four-centered transition state (**D5TS**).

It is seen in Table 1 that the inclusion of correlation effects decreases the energy barrier (ΔE, **D2TS**) of the first step significantly. The B3LYP/6-31+G* and MP2/6-31+G** levels of theory both predict an activation barrier that is about 16 kcal/mol lower than that of the HF/6-31+G* level. The zero-point vibrational energy correction (ΔZPVE) lowers the barrier by 2.8 kcal/mol, while the thermal contributions to the enthalpy correction ($\Delta\Delta H_g$) and the free energy correction ($\Delta\Delta G_g$) have little effect on the barrier height. The relative energy of **D3** is also lower with the B3LYP and MP2 methods than with the HF method. This is, at least partly, a consequence of the importance of electron correlation for describing hydrogen bonds. Accordingly, it is seen in Figure 1 that the B3LYP optimized hydrogen bonds in **D3** are shorter than those from the HF optimization. It can also be noted that the formation of **D3** from **1** is entropically favored by as much as 4.7 kcal/mol at 298 K (compare $\Delta\Delta H_g$ and $\Delta\Delta G_g$). The exchange of methanol for water, i.e., going from **D3** to **D4**, is energetically favored by 1.7 kcal/mol at the B3LYP/6-31+* level. This is reduced to 0.9 kcal/mol after the free energy correction. The second transition state (**D5TS**) is both structurally and energetically very similar to the first (**D2TS**). Finally, the overall reaction, going from **1** to the product **D6**, is almost thermoneutral at the B3LYP/6-31+G* level. The overall free energy change is also close to zero at the same level, while the MP2 results suggests a slightly positive change.

Turning to the free energies in solution ($\Delta G°_{aq}$), Table 1 shows that solvation effects destabilizes **D2TS** by 4.2 kcal/mol. Complex **D3** is even more destabilized in solution, 10.2 kcal/mol relative to **1**. This is not surprising considering the more delocalized negative charge in **D3** compared to **1**. It is more unexpected that the solvation free energy ($\Delta\Delta G_{PCM}$) of complex **D4** is 2.5 kcal/mol higher than that of complex **D3**. The reason for this seems to be that the negative charge of PO_3^- is better shielded from the solvent in **D4** than in **D3**, since the water molecule in **D4** is bonded to PO_3^- by two hydrogen bonds, whereas in **D3** the methanol only binds to PO_3^- with one hydrogen bond. However, this result may be an artifact of the computational approach we have used. It is likely that each water molecule in the first solvation shell of solvated PO_3^- forms only one hydrogen bond with the solute and that the second hydrogen binds to the solvent. To get a better description of the hydrogen bonds in the solvation shell, it would be necessary to optimize the geometry with PCM, or preferably work with a much larger cluster. The reason that the exchange of water for methanol (going from **D3** to **D4**), despite the unfavorable solvation effect, is favored is the gain of −2.4 kcal/mol in free energy that stems from the difference in concentration between water and methanol. (The standard state corresponds to 55 M water and 1 M methanol). After consideration of solvation effects, **D5TS** is 1.4 kcal/mol lower in free energy than **D2TS**. The total change in free energy for the reaction (going from **1** to **D6**) is −1.6 kcal/mol. This is in good agreement with an indirect estimate of Guthrie, −2 kcal/mol, which is based on experimental data for similar species.[35]

2. Reaction of $CH_3OPO_3H^-\cdot(H_2O)$. For the $CH_3OPO_3H^-\cdot(H_2O)$ species, both the dissociative and associative mechanisms are possible. We have followed both reaction pathways and have illustrated the structures of the stationary points in Figure 2. Both pathways begin with the $CH_3OPO_3H^-\cdot(H_2O)$ complex (**11**). In the dissociative mechanism, one big difference compared with the $CH3OPO_3H^-$ reaction is that the $PO_3^-\cdot CH_3OH\cdot H_2O$ complex (**D13**) can be formed either via a four-centered (**D12bTS**) or a six-centered water-assisted transition state (**D12aTS**). Note that the formation of **D12aTS** is not likely to

TABLE 1: Relative Energies (kcal/mol) of the Stationary Points for the Reaction of $CH_3OPO_3H^-$[a]

	HF[b]	B3LYP[c]	MP2[d]	ΔZPVE	$\Delta\Delta H_g$	$\Delta\Delta G_g$	$\Delta\Delta G_{PCM}$	$\Delta G°_g$	$\Delta G°_{aq}$
1	0.0	0.0	0.0	0.0	0.0	0.0	0.0	0.0	0.0
					Dissociative Mechanism				
D2TS	49.7	33.1	33.6	−2.8	−2.9	−2.9	4.2	30.7	34.5
D3	17.9	10.4	13.5	−0.7	0.2	−4.5	10.2	6.4	16.5
D4	16.3	8.7	12.1	0.3	0.5	−3.2	12.7	5.5	15.8
D5TS	50.1	33.5	36.6	−1.5	−2.4	−3.0	5.0	30.5	33.1
D6	−0.5	−0.1	2.1	1.0	0.4	−0.3	1.2	−0.4	−1.6

[a] The definitions for the energetics (with respect to the minimum **1**) are: ΔE, classical energy; ΔZPVE, zero-point vibrational energy; $\Delta\Delta H$, enthalpy correction; $\Delta\Delta G_g$, free energy correction; $\Delta\Delta G_{PCM}$, PCM solvation free energy correction; $\Delta G°_g = \Delta E$(B3LYP) + $\Delta\Delta G_g$, $\Delta G°_{aq} = \Delta G°_g + \Delta\Delta G_{PCM}$. $\Delta\Delta H_g$ and $\Delta\Delta G_g$ are calculated at 298 K and 1 atm, with the vibrational frequencies obtained at the HF/6-31+G* level (scaled by 0.89). For the points **4**−**6**, −2.4 kcal/mol [$-RT$ ln(55)] has been added to the $\Delta G°_{aq}$ values, since the standard state corresponds to 1 M aqueous solution and liquid water (55 M H_2O). [b] ΔE calculated at the HF/6-31+G*//HF/6-31+G* level of theory. [c] ΔE calculated at the B3LYP/6-31+G*//B3LYP/6-31+G* level of theory. [d] ΔE calculated at the MP2/6-31+G**//B3LYP/6-31+G* level of theory.

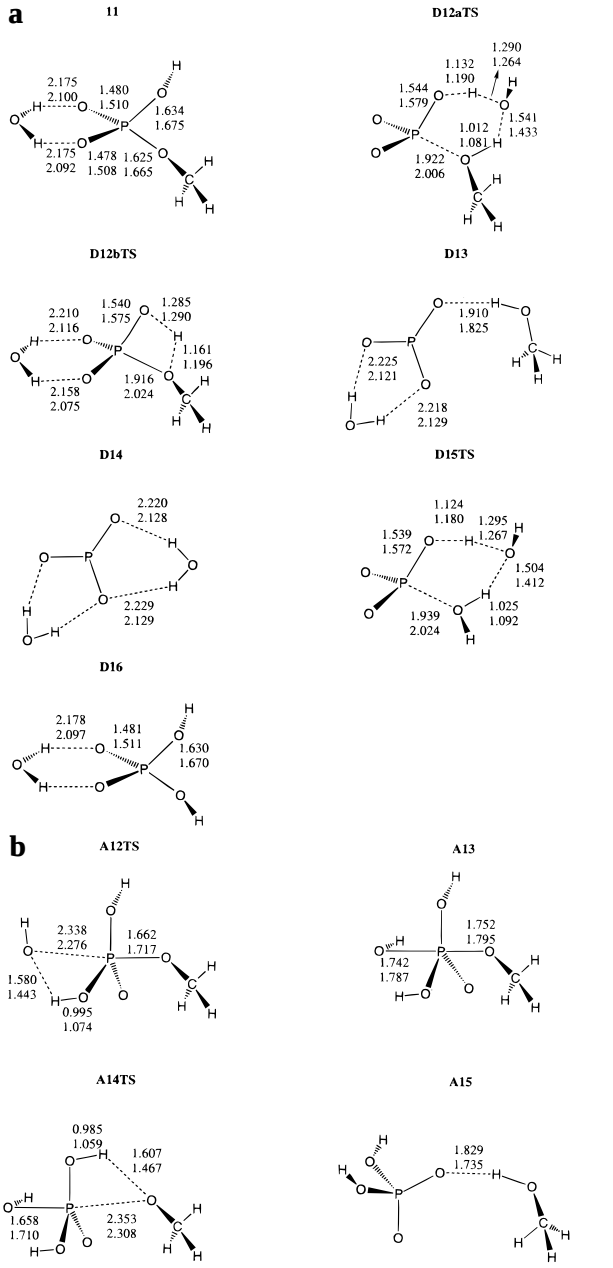

Figure 2. Structures of the stationary points involved in the reaction of $CH_3OPO_3H^-\cdot(H_2O)$. The first and second entries of the selected bond lengths (in Å) are computed at the HF/6-31+G* and B3LYP/6-31+G* levels of theory, respectively. (a) Structures associated with the dissociative mechanism. (b) Structures associated with the associative mechanism. Note that the reaction begins with structure **11**, which is shown in Figure 2a.

be a one-step process. The water molecule in **11** needs to alter its location before **D12aTS** can be formed and this process is likely to proceed via a barrier. However, this barrier is expected to be small, in particular when compared with the overall barrier for the reaction. Also, the isomerization of **D14** can, in principle, proceed via either a four-centered or a six-centered transition state. However, earlier theoretical studies have shown the six-centered transition state (**D15TS**) to be energetically favored.[12,13] In the associative mechanism, the water molecule attacks the phosphorus atom via **A12TS** and forms the TBP complex **A13**. The next step is a proton transfer to the methoxy oxygen (**A14TS**), yielding the $H_2PO_4^-\cdot(CH_3OH)$ complex **A15**.

The gas phase results in Table 2 show that the dissociative mechanism is much more favorable than the associative mechanism. At the B3LYP/6-31+G* and MP2/6-31+G** levels of theory, **D12aTS** is lower in energy than **A12TS** by approximately 15 kcal/mol, and it is about 17 kcal/mol lower in free energy. In the first step of the dissociative mechanism, the six-centered transition state is favored over the four-centered by 6.6 kcal/mol at the B3LYP/6-31+G* level. The difference decreases after consideration of entropy effects. However, there is still a difference of 4.8 kcal/mol in the free energy at 298 K. The second transition state in the dissociative mechanism is very similar in free energy to the first; the difference is only 0.9 kcal/mol. The exchange of methanol for water in **D13** to form **D14** is enthalpically favored by 1.3 kcal/mol, but disfavored in free energy terms by 0.3 kcal/mol due to the negative change in entropy. The overall free energy change of the reaction is −1.0 kcal/mol, which is only 0.6 kcal/mol lower than free energy change in the reaction of the $CH_3OPO_3H^-$ species. In the associative mechanism, the second transition state (**A14TS**) is of lower energy than the first (**A12TS**) in the gas phase; the free energy difference is 3.5 kcal/mol. It has to be noted that we have only presented the inline attack reaction path in the associative mechanism. Due to the character of the geometry of **A12TS**, the TBP intermediate (**A13**) has an inline structure and therefore does not have to undergo pseudorotations before completing the reaction. We have optimized the two noninline intermediates at the HF/6-31+G* level. It was found that these two intermediates are 5 and 17 kcal/mol higher in energy than the inline one.

The difference in free energy of activation between the dissociative mechanism and the associative mechanism is reduced after the inclusion of PCM solvation energies. However, the difference is still considerable, 12.1 kcal/mol. Thus, the calculations clearly favor the dissociative mechanism over the associative mechanism also in solution. In contrast to the gas phase free energies, the $\Delta G°_{aq}$ value for **A12TS** is lower than that for **A14TS**. It is not surprising that the solvent has a large stabilizing effect on **A12TS** considering that it contains a nearly bare OH^- anion. In contrast, the two transition states in the dissociative mechanism, **D12aTS** and **D15TS**, remain very similar in free energy also after consideration of solvation effects. The inclusion of solvation effects increases the energy difference between the four- and six-centered transition states of the dissociative mechanism. The $\Delta G°_{aq}$ values are 33.5 and 23.7 kcal/mol for **D12bTS** and **D12aTS**, respectively. It is interesting to note that the $\Delta G°_{aq}$ values for the four-centered transition state in the reactions of $CH_3OPO_3H^-$ and $CH_3OPO_3H^-\cdot(H_2O)$ differ by only 1.1 kcal/mol. For the complexes, **D3** and **D13**, the $\Delta G°_{aq}$ values are identical. It is indeed encouraging that the addition of water molecules that do not take an active part in the reaction does not significantly influence the final $\Delta G°_{aq}$ values. However, as we noted when discussing the results for the $CH_3OPO_3H^-$ species, the computational approach taken seems to have some problem in describing the exchange of methanol for water that follows the PO_3^- formation, i.e., going from **D13** to **D14**. The $\Delta\Delta G_{PCM}$ value for this process is 2.6 kcal/mol, which is almost identical to that of going from **D3** to **D4**. This value together with the negative entropy effect leads to a change in free energy in solution for the process of going from **D3** to **D4** that is slightly positive. The change in free energy for the overall reaction (**11** to **D16**) is −2.5 kcal/mol, which is only 0.9 kcal/mol lower than for the reaction of the $CH_3OPO_3H^-$ species.

3. Reaction of $CH_3OPO_3H^-\cdot(H_2O)_2$. The structures of the stationary points involved in the reaction of the $CH_3OPO_3H^-\cdot(H_2O)_2$ species are shown in Figure 3. The energetics is

TABLE 2: Relative Energies (kcal/mol) of the Stationary Points for the Reaction of $CH_3OPO_3H^-\cdot H_2O$[a]

	HF	B3LYP	MP2	ΔZPVE	$\Delta\Delta H_g$	$\Delta\Delta G_g$	$\Delta\Delta G_{PCM}$	ΔG°_g	ΔG°_{aq}
11	0.0	0.0	0.0	0.0	0.0	0.0	0.0	0.0	0.0
					Dissociative Mechanism				
D12aTS	46.1	27.5	27.5	−2.5	−3.4	−0.8	−2.9	26.7	23.8
D12bTS	50.6	34.1	34.4	−2.6	−2.8	−2.6	1.9	31.5	33.4
D13	20.5	13.0	16.1	−0.9	0.2	−5.1	8.6	7.9	16.5
D14	19.0	11.5	14.9	0.1	0.4	−3.3	11.2	8.2	17.0
D15TS	47.3	29.3	32.1	−1.6	−3.3	−1.7	−1.6	27.6	23.6
D16	−0.6	−0.1	2.1	0.8	0.3	−0.9	0.9	−1.0	−2.5
					Associative Mechanism				
A12TS	54.2	42.6	43.0	−0.8	−1.7	1.2	−7.7	43.8	36.1
A13	37.8	30.8	29.9	1.3	0.3	3.6	−3.1	34.4	31.3
A14TS	49.9	40.0	41.4	−1.2	−1.9	0.2	−2.6	40.2	37.6
A15	0.7	1.0	3.9	−0.1	0.1	−2.6	−1.2	−1.6	−2.8

[a] Refer to the end of Table 1 for definition of the thermodynamic quantities.

summarized in Table 3. The stationary points illustrated in Figure 3 correspond to those in Figure 2 with an extra water molecule, i.e., **21** corresponds to **11** plus H_2O, etc. The formations of the transition states **D22bTS**, **D22aTS**, and **A22TS** from **21**, and **D25TS** from **D24**, require rearrangements of the water molecules. These processes are not necessarily barrierless. However, compared with the overall reaction barriers these barriers are certainly small. It should be noted that we have not been able to locate any six-centered transition states for the associative mechanism. All our efforts to optimize such a transition state resulted in a return to one of the four-centered transition states (**A22TS** or **A24TS**). The reason for this behavior seems to be that the pentacoordinated oxygens are too close in space which makes a six-centered transition state too crowded and strained.

The general trend in the gas phase reaction energies of the $CH_3OPO_3H^-\cdot(H_2O)_2$ species is similar to the $CH_3OPO_3H^-\cdot(H_2O)$ species. The dissociative pathway that proceeds via six-centered water-assisted transition state (**D22aTS**) in the first step is also here the most favorable mechanism. Compared to the $CH_3OPO_3H^-\cdot(H_2O)$ species, the free energy of the second transition state (**D25TS**) in the dissociative mechanism is reduced by 3.3 kcal/mol. Relative to the hydrated PO_3^- (**D24a**), the lowering in the free energy of **D25TS** is even bigger; the activation free energy for forming $H_2PO_4^-$ from PO_3^- is reduced from 19.4 to 13.4 kcal/mol when going from the $PO_3^-\cdot(H_2O)_2$ to the $PO_3^-\cdot(H_2O)_3$ cluster. This result is consistent with the experimental observation that $PO_3^-\cdot(H_2O)_2$ clusters are stable in the gas phase, while the addition of an extra water molecules results in rapid isomerization to $H_2PO_4^-\cdot(H_2O)_2$. The reason for this extra stabilization of **D25TS** compared to **D15TS** is the formation of an additional six-centered ring in which the added water molecule is hydrogen bonded to both the PO_3^- and the attacking water. A similar ring structure is not possible in the first transition state of the dissociative mechanism, since the leaving group, methanol, cannot form a suitable hydrogen bond to the water. On the basis of Hartree−Fock calculations, Wu and Houk have suggested that structure **D24b** is the dominant geometry of $PO_3^-\cdot(H_2O)_2$.[13] However, our B3LYP/6-31+G* calculations show that this structure is 2.6 kcal/mol higher in electronic energy (ΔE) and 6.8 kcal/mol higher in free energy than **D24a**.[36] It should be noted that structure **D24b** is not a stable minimum at the HF/6-31+G* level. Wu and Houk used smaller basis sets than 6-31+G* in their calculations,[13] and thus the large stability of **D24b** was probably an effect of large basis set superposition errors. In the associative mechanism, we find the largest difference between $CH_3OPO_3H^-\cdot(H_2O)_2$ and $CH_3OPO_3H^-\cdot(H_2O)$ species in the activation energy of the first step; the inclusion of an extra water molecule leads to a reduction in the free energy of activation by 4.6 kcal/mol. This extra stabilization of **A22TS** is consistent with the large stabilizing effect of PCM solvation on **A12TS**.

Looking at the results of the PCM calculations for the $CH_3OPO_3H^-\cdot(H_2O)_2$ species, we note that the relative solvation energies ($\Delta\Delta G_{PCM}$) generally are smaller in magnitude than for the $CH_3OPO_3H^-\cdot(H_2O)$ species. However, the resulting relative free energies in solution (ΔG°_{aq}) for the two data sets are in most cases in good agreement with each other. For example, the difference in ΔG°_{aq} between **A22TS** and **A12TS** is only 0.4 kcal/mol, despite the large difference in ΔG°_g. In contrast, the difference in free energy between **D25TS** and **D15TS** is not significantly reduced by the inclusion of PCM solvation. It is not surprising that specific hydrogen bond interactions of the type present in **D25TS** cannot be accounted for by the PCM method. The difference in ΔG°_{aq} between **D25TS** and **D24a**, the hydrated PO_3^-, is only 1.5 kcal/mol, which suggest that PO_3^- reacts very rapidly in solution. However, as we have discussed earlier, a structure like **D24a** where each water molecule is hydrogen bonded to two oxygens from PO_3^- is not likely to be representative for the structure in solution.

Discussion

Our results for the reactions of the $CH_3OPO_3H^-\cdot(H_2O)$ and the $CH_3OPO_3H^-\cdot(H_2O)_2$ species strongly suggest that the dissociative mechanism is the dominating pathway for hydrolysis of the methyl phosphate anion in solution. The fact that the computed solution activation energies for the two species are in good agreement indicates that the approach of combining explicit water molecules with a PCM solvation model is sound. It also suggests that the results will not change dramatically if additional water molecules are included in the calculations. In addition, it does not seem likely that more than two water molecules play a catalytic role in the reaction, since this would be entropically very unfavorable.

The computed activation energy for the dissociative mechanism is surprisingly low. On the basis of the experimental rate constant (8×10^{-6} s^{-1} at pH 4.2) and traditional transition-state theory, we estimate the free energy of activation to 30.7 kcal/mol at 373 K. This is more than 6 kcal/mol higher than our computed activation energy for the $CH_3OPO_3H^-\cdot(H_2O)$ species (ΔG°_{aq} for **12aTS** is 24.4 at 373 K). Since the B3LYP method has been reported to underestimate activation energies for several types of reactions,[24,25] we decided to investigate if high-level ab initio computations can provide energies in better agreement with experiment. Energies for structures **11**, **D12aTS**,

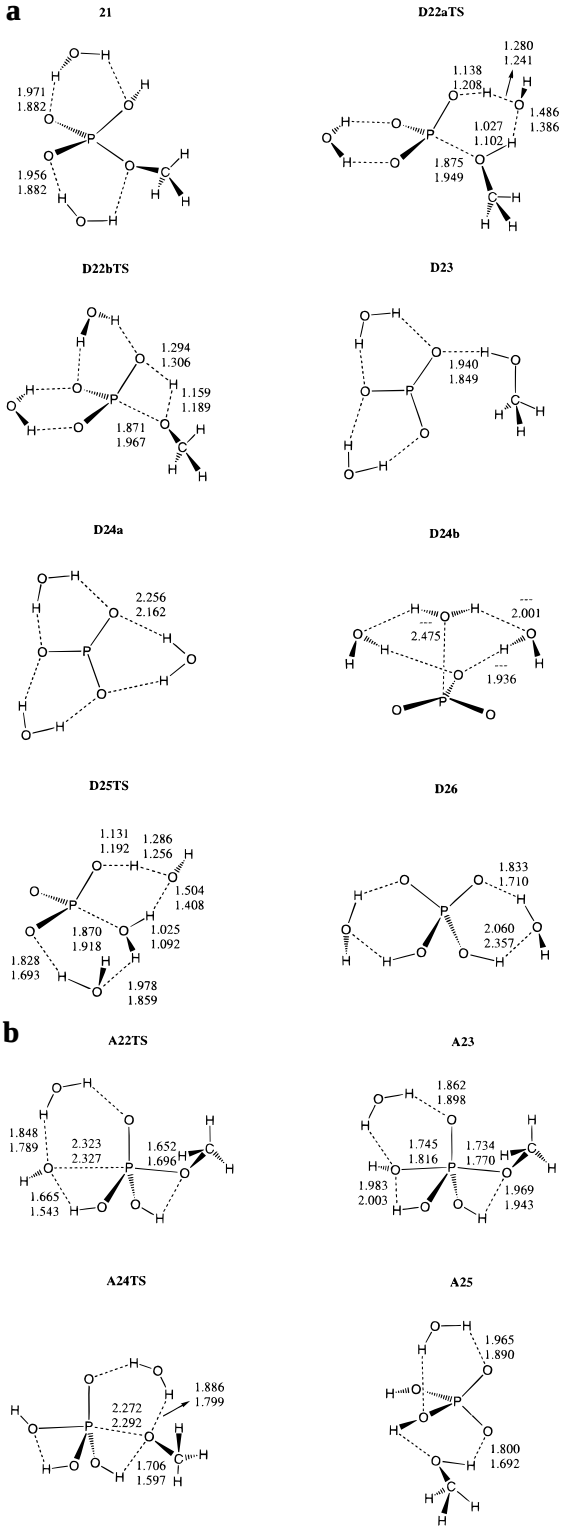

Figure 3. Structures of the stationary points involved in the reaction of $CH_3OPO_3H^-\cdot(H_2O)_2$. The first and second entries of the selected bond lengths (in Å) are computed at the HF/6-31+G* and B3LYP/6-31+G* levels of theory, respectively. (a) Structures associated with the dissociative mechanism. Note that structure **D24b** is not a stable minimum at the HF/6-31+G* level. (b) Structures associated with the associative mechanism. Note that the reaction begins with structure **21**, which is shown in Figure 3a.

D15TS, **A12TS**, and **A14TS** were computed using different methods and the 6-31+G* basis set. MP2 theory was used to investigate the influence of the basis set on the relative energies. As can be seen in Table 4, the relative energy of **D12aTS** depends rather strongly on the computational method. The most sophisticated method, CCSD(T), gives an activation energy that is 4.2 kcal/mol higher than the B3LYP value obtained with the same basis set (6-31G*). There is also a significant basis set effect on the activation energy; the relative energy of **D12aTS** at the MP2/6-311+G(2df,2p) level is 0.4 kcal/mol higher than at the MP2/6-31+G* level, which in turn is 1.6 kcal/mol higher than the MP2/6-31G** energy (see Table 2). By combining the MP2 energies with the CCSD(T) energy according to eq 1, we estimate the gas phase activation energy of the dissociative mechanism to 32.1 kcal/mol. After vibrational correction and addition of PCM solvation energies, this corresponds to an activation free energy in solution of 29.0 kcal/mol at 373 K. Thus, there is only a difference of 1.7 kcal/mol between our best computed activation energy and the estimate based on the experimental rate constant (30.7 kcal/mol). This is indeed a very encouraging result considering the difficulties of estimating the solvent effects on the reaction. The second transition state (**D15TS**) is only 0.6 kcal/mol lower in free energy than **D12TS**. However, as we have discussed, this transition state is significantly stabilized by the introduction of an additional water molecule. Looking at the relative energy of structure **A12TS**, which corresponds to the activation energy of the first step in the associative mechanism, we note a smaller dependence upon the choice of method than for the energies of structures **D12aTS** and **D15TS**. The activation energy at the CCSD(T)/6-31+G* level is only 2.4 kcal/mol higher than at the B3LYP/6-31+G* level. The difference decreases to 1.4 kcal/mol after addition of the MP2 basis set correction to the CCSD(T) energy (eq 1). The final estimate of the activation free energy in solution for the first step in the associative mechanism is 38.3 kcal/mol at 373 K. This is 7.6 kcal/mol higher than the estimated experimental activation free energy for hydrolysis. In addition, the second transition state (**A14TS**) in the associative mechanism is 0.9 kcal/mol higher in energy than the first (**A12TS**) after the solvation correction. Thus, our computational results suggest that the overall activation free energy for the associative mechanism is more than 8 kcal/mol higher than the activation energy estimated from the experimental rate constant for hydrolysis. Whereas our computational activation energies might be in error by a few kcal/mol due to the problem with treatment of solvent effects, this cannot account for such a large discrepancy between the computational and experimental results. Our conclusion is therefore that the associative mechanism plays only a minor role in the hydrolysis of the methyl phosphate anion.

It should be noted that our computed activation barriers for the associative mechanism are in relatively good agreement with the barriers computed by Florian and Warshel.[16] Our best estimates of the relative free energies for the first and second transition states are 37.5 and 38.6 kcal/mol, respectively, in solution at 298 K. The corresponding values from the study of Florian and Warshel are 34.5 and 38.3 kcal/mol.[16] Since they did not consider the possibility of six-centered water-assisted transition states in the dissociative mechanism, their computed transition state free energies for this mechanism are considerably higher than ours. However, if the comparison is made with our results for the four-centered transition state, the agreement is considerably better; their calculated free energy for the first transition state in the dissociative mechanism is 33.6 kcal/mol, while our calculations give a free energy that varies between 33.3 and 34.5 kcal/mol depending on the cluster size (see Tables 1−3). Since Florian and Warshel used a rather different approach for treating solvation effects, the good agreement

TABLE 3: Relative Energies (kcal/mol) of the Stationary Points for the Reaction of $CH_3OPO_3H^-\cdot(H_2O)_2$[a]

	HF	B3LYP	MP2	ΔZPVE	ΔΔ*H*	$\Delta\Delta G_g$	$\Delta\Delta G_{PCM}$	ΔG°_g	ΔG°_{aq}
21	0.0	0.0	0.0	0.0	0.0	0.0	0.0	0.0	0.0
				Dissociative Mechanism					
D22aTS	45.3	26.8	27.0	−2.4	−3.5	−0.4	−2.1	26.4	24.3
D22bTS	50.5	34.8	35.0	−2.3	−2.7	−1.8	0.2	33.0	33.2
D23	22.3	15.4	18.9	−0.8	0.2	−4.6	8.1	10.8	18.9
D24a	23.2	14.1	18.9	0.1	0.3	−3.0	10.3	11.1	19.0
D25TS	43.4	24.8	29.4	−0.7	−2.9	−0.5	−1.4	24.3	20.5
D26	0.3	−1.6	2.3	1.6	0.6	0.0	0.0	−1.6	−4.0
				Associative Mechanism					
A22TS	46.4	35.9	37.0	−0.2	−1.1	3.3	−2.7	39.2	36.5
A23	36.6	29.1	28.5	1.4	0.3	3.9	−1.3	33.0	31.7
A24TS	45.8	35.9	37.0	0.0	−1.3	2.9	0.6	38.8	39.4
A25	0.0	−0.9	1.4	0.6	0.3	0.5	−0.1	−0.4	−0.5

[a] Refer to end of Table 1 for the definition of the thermodynamic quantities.

TABLE 4: Energies (kcal/mol) of Activation for the Reaction of $CH_3OPO_3H^-\cdot(H_2O)$

	B3LYP/ 6-31+G*[a]	MP2/ 6-31+G*[a]	MP2/ 6-311+G(2df,2p)[a]	CCSD(T)/ 6-31+G*[a]	CCSD(T)/ (G2X)[b]	ΔG°_g (298 K)[c]	ΔG°_{aq} (298 K)[d]	ΔG°_{aq} (373 K)[e]
11	0.0	0.0	0.0	0.0	0.0	0.0	0.0	0.0
			Dissociative Mechanism					
D12aTS	27.5	28.7	29.1	31.7	32.1	31.3	28.4	29.0
D15TS	29.3	33.0	32.8	34.5	34.3	32.6	28.6	28.4
			Associative Mechanism					
A12TS	42.6	44.3	43.3	45.0	44.0	45.2	37.5	38.3
A14TS	40.0	42.8	40.6	43.2	41.0	41.2	38.6	39.2

[a] Δ*E* calculated at the denoted level of theory using B3LYP/6-31+G* optimized geometries. [b] ΔE[CCSD(T)/(G2X)] = ΔE[MP2/6-311+G(2df,2p)] − ΔE[MP2/6-31+G*] + ΔE[CCSD(T)/6-31+G*]. [c] $\Delta G_g(298\text{ K}) = \Delta E[\text{CCSD(T)/(G2X)}] + \Delta\Delta G_g(298\text{ K})$. [d] $\Delta G^\circ_{aq}(298\text{ K}) = \Delta E[\text{CCSD(T)/(G2X)}] + \Delta\Delta G_{PCM} + \Delta\Delta G_g(298\text{ K})$. For **25TS**, −2.4 kca/mol [$-RT$ ln(55)] has been added to $\Delta G^\circ_{aq}(298\text{ K})$ to correct for the standard state of 1 M aqueous solution and liquid water (55 M H_2O). [e] $\Delta G^\circ_{aq}(373\text{ K}) = \Delta E[\text{CCSD(T)/(G2X)}] + \Delta\Delta G_{PCM} + \Delta\Delta G_g(373\text{ K})$. For **25TS**, −3.0 kca/mol [$-RT$ ln(55)] has been added to $\Delta G^\circ_{aq}(373\text{ K})$ to correct for the standard state of 1 M aqueous solution and liquid water (55 M H_2O).

between the two studies can be seen as a support for the results obtained in this work.

As we discussed in the Introduction, Florian and Warshel have suggested that the TBP intermediate (**A13** or **A23**) may be formed in a two-step process where the phosphate anion first abstracts a proton from a water molecule followed by an attack of the formed OH^- on the now protonated phosphate.[17] However, as has been pointed out by these authors, the important transition states for the regular associative mechanism and "OH^- attack mechanism" are likely to be very similar.[16] Consequently, the two mechanisms are expected to have similar activation energies. Since we have found the dissociative mechanism to be strongly favored over the associative mechanism, the conclusion must be that the OH^- attack mechanism is not of any greater importance for the hydrolysis of the methyl phosphate anion.

Summary and Conclusions

In this work we have studied the mechanism for ester hydrolysis of the methyl phosphate anion by quantum chemical calculations on the molecular species, $CH_3OPO_3H^-$, $CH_3OPO_3H^-\cdot(H_2O)$, and $CH_3OPO_3H^-\cdot(H_2O)_2$. After the addition of PCM solvation energies, the free energies of the transition states for the investigated mechanisms vary only slightly between the different species. Only in those cases where the added water molecule plays an active catalytic role in the transition state do the free energy change significantly with an increase of the cluster size. These results suggest that the computational approach we have used is sound and that the solvation effects are properly accounted for.

Our highest level computations show that the dissociative mechanism is favored over the associative by more than 10 kcal/mol of free energy in solution. The computed free energy of activation for the dissociative mechanism is within 1.7 kcal/mol of the experimentally determined activation free energy for hydrolysis. In this mechanism, the first step is found to be rate determining. The first step and the second step are each shown to proceed via a six-centered water-assisted transition state. However, in the second step transition state there is an additional tightly bound water molecule that provides extra stabilization. The two transition states in the associative mechanism are both four-centered. The reason for this seems to be that the pentacoordinated oxygens are so close in space that a six-centered transition state would become too crowded and strained.

Acknowledgment. We thank Dr. Gabor Merenyi for many fruitful discussions. The Swedish Natural Science Research Council (NFR) and the Faculty of Chemistry and Chemical Engineering at the Royal Institute of Technology are gratefully acknowledged for financial support. This work was supported with computing resources by the Swedish Council for Planning and Coordination of Research (FRN) and Paralelldatorcentrum (PDC), Royal Institute of Technology.

References and Notes

(1) Westheimer, F. H. *Science* **1987**, *235*, 1173.

(2) Bunton, C. A.; Llewellyn, D. R.; Oldham, K. G.; Vernon, C. A. *J. Chem. Soc.* **1958**, 3574.

(3) Butcher, W. W.; Westheimer, F. H. *J. Am. Chem. Soc.* **1955**, *77*, 2420.

(4) Barnard, P. W. C.; Bunton, C. A.; Llewellyn, D. R.; Oldham, K. G.; Silver, B. L.; Vernon, C. A. *Chem. Ind. (London)* **1955**, 760.

(5) Jencks, W. P. *Acc. Chem. Res.* **1980**, *13*, 161.

(6) Bourne, N.; Williams, A. *J. Am. Chem. Soc.* **1984**, *106*, 7591.

(7) Skoog, M. T.; Jencks, W. P. *J. Am. Chem. Soc.* **1984**, *106*, 7597.

(8) Ramirez, R.; Marecek, J.; Minore, J.; Srivastava, S.; le Noble, W. *J. Am. Chem. Soc.* **1986**, *108*, 348.
(9) Herschlag, D.; Jencks, W. P. *J. Am. Chem. Soc.* **1990**, *112*, 1951.
(10) Lightcap, E. S.; Frey, P. A. *J. Am. Chem. Soc.* **1992**, *114*, 9750.
(11) Keesee, R. G.; Castleman, A. W. J. *J. Am. Chem. Soc.* **1989**, *111*, 9015.
(12) Ma, B.; Xie, Y.; Shen, M.; Schleyer, P. v. R.; Schaefer, H. F. *J. Am. Chem. Soc.* **1993**, *115*, 11169.
(13) Wu, Y.-D.; Houk, K. N. *J. Am. Chem. Soc.* **1993**, *115*, 11997.
(14) Westheimer, F. H. *Acc. Chem. Res.* **1968**, *1*, 70.
(15) Westheimer, F. H. *Chem. Rev.* **1981**, *81*, 313.
(16) Florian, J.; Warshel, A. *J. Phys. Chem. B* **1998**, *102*, 719.
(17) Florian, J.; Warshel, A. *J. Am. Chem. Soc.* **1997**, *119*, 5473.
(18) Becke, A. D. *J. Chem. Phys.* **1993**, *98*, 5648.
(19) Lee, C.; Yang, W.; Parr, R. G. *Phys. Rev. B* **1988**, *37*, 785.
(20) Martin, J. M. L.; El-Yazal, J.; Francois, J.-P. *Mol. Phys.* **1995**, *86*, 1437.
(21) Curtiss, L. A.; Raghavachari, K.; Redfern, P. C. *J. Chem. Phys.* **1997**, *106*, 1063.
(22) Martell, J. M.; Goddard, J. D.; Eriksson, L. A. *J. Phys. Chem.* **1997**, *101*, 1927.
(23) Wiest, O.; Black, K. A.; Houk, K. N. *J. Am. Chem. Soc.* **1994**, *116*, 10336.
(24) Zhang, Q.; Bell, R.; Truong, N. *J. Phys. Chem.* **1995**, *99*, 592.
(25) Durant, J. L. *Chem. Phys. Lett.* **1996**, *256*, 595.
(26) Goldstein, E.; Beno, B.; Houk, K. N. *J. Am. Chem. Soc.* **1996**, *118*, 6036.
(27) Curtiss, L. A.; Redfern, P. C.; Smith, B. J.; Radom, L. *J. Chem. Phys.* **1996**, 5148.
(28) Durant, J. L.; Rohlfing, C. M. *J. Chem. Phys.* **1993**, *98*, 8031.
(29) Jungkamp, T. P. W.; Seinfeld, J. H. *J. Chem. Phys.* **1997**, *107*, 1513.
(30) Cossi, M.; Barone, V.; Cammi, R.; Tomasi, J. *Chem. Phys. Lett.* **1996**, *255*, 327.
(31) Schmidt, M. W.; Baldridge, K. K.; Boatz, J. A.; Elbert, S. T.; Gordon, M. S.; Jensen, J. H.; Koseki, S.; Matsanuga, N.; Nguyen, K. A.; Su, S. J.; Windus, T. L.; Dupuis, M.; Montgomery, J. A. *J. Com. Chem.* **1993**, *14*, 1347.
(32) Mennucci, B.; Tomasi, J. *J. Chem. Phys.* **1997**, *106*, 5151.
(33) Tomasi, J.; Persico, M. *Chem. Rev.* **1994**, *94*, 2027.
(34) Frisch, M. J.; Trucks, G. W.; Schlegel, H. B.; Gill, P. M. W.; Johnson, B. G.; Robb, M. A.; Cheeseman, J. R.; Keith, T. A.; Petersson, G. A.; Montgomery, J. A.; Raghavachari, K.; Al-Laham, M. A.; Zakrzewski, V. G.; Ortiz, J. V.; Foresman, J. B.; Peng, C. Y.; Ayala, P. Y.; Chen, W.; Wong, M. W.; Andres, J. L.; Replogle, E. S.; Gomperts, R.; Martin, R. L.; Fox, D. J.; Binkley, J. S.; Defrees, D. J.; Baker, J.; Gonzalez, C.; Stewart, J. J. P.; Head-Gordon, M.; Pople, J. A. *Gaussian 94, Rev. B.3*; Gaussian, Inc.: Pittsburgh, PA, 1995.
(35) Guthrie, J. P. *J. Am. Chem. Soc.* **1977**, *99*, 3991.
(36) The free energy difference has been calculated using unscaled B3LYP/6-31+G* frequencies, since structure **D24b** is not a minimum at the HF/6-31+G* level.